Eur. Phys. J. B **23**, 57–67 (2001)

THE EUROPEAN PHYSICAL JOURNAL B

EDP Sciences

Competition of disorder and interchain hopping in a two-chain Hubbard model

E. Orignac[1,a] and Y. Suzumura[2]

[1] LPTENS[b] 24, rue Lhomond 75231 Paris Cedex 05, France
[2] Department of Physics, Nagoya University, Nagoya 464-8602, Japan
and
CREST, Japan Science and Technology Corporation (JST), Japan

Received 6 April 2001

Abstract. We study the interplay of Anderson localization and interaction in a two chain Hubbard ladder allowing for arbitrary ratio of disorder strength to interchain coupling. We obtain three different types of spin gapped localized phases depending on the strength of disorder: a pinned $4k_F$ Charge Density Wave (CDW) for weak disorder, a pinned $2k_F$ CDW$^\pi$ for intermediate disorder and two independently pinned single chain $2k_F$ CDW for strong disorder. Confinement of electrons can be obtained as a result of strong disorder or strong attraction. We give the full phase diagram as a function of disorder, interaction strength and interchain hopping. We also study the influence of interchain hopping on localization length and show that localization is enhanced by a small interchain hopping but suppressed by a large interchain hopping.

PACS. 71.10.Pm Fermions in reduced dimensions (anyons, composite fermions, Luttinger liquid, etc.) – 71.23.An Theories and models; localized states

1 Introduction

In the recent years, the two-chain Hubbard model received a lot of theoretical attention both analytically [1–11] and numerically [12–19]. The outcome of these studies was that the two-chain Hubbard model with repulsive interactions would present a metallic phase with a spin gap containing dominant "d-wave" superconducting fluctuations, a situation very reminiscent of the situation in two-dimensional cuprate superconductors. This result leads to the conjecture that the two-chain Hubbard model could be considered as a toy-model of cuprate superconductivity. More recently, experiments revealed that the material with two-chain structure $Sr_{14}Cu_{24}O_{41}$ doped with Ca could become metallic [20] and displayed a superconducting phase under pressure. This superconducting phase has been interpreted as the stabilization of "d-wave" fluctuations by interladder Josephson coupling. Such an interpretation is not clear enough because doping by Ca is not only introducing carriers in the system, but also inducing disorder.

In a one-dimensional system, even an infinitesimal disorder induces Anderson localization and an insulating state in the presence of interactions [21]. Therefore it is crucial to understand the effect of interchain coupling on Anderson localization. At present, the effect of an infinitesimal disorder in the limit of strong interchain coupling has been analyzed [22,23]. The outcome of this study is that although the presence of the spin-gap suppresses the coupling of disorder to $2k_F$ fluctuations, disorder can still couple to $4k_F$ fluctuations (k_F being the Fermi wave vector) leading to an insulating phase rather than a superconducting phase at low temperature. Indeed, there is some experimental evidence from transport measurements [24–27] that the phase at low temperature under ambient pressure is a pinned Charge Density Wave (CDW) state. This, as well as the disappearance of spin gap in NMR and the reduction of anisotropy of electrical conductivity close to the superconducting transition has lead to the idea that pressure could cause a dimensional crossover from 1D insulator to 2D superconductor and that superconductivity in this system is intrinsically two-dimensional phenomenon [28–31]. Building on the results of [23], a phenomenological theory of transport in the insulating state of the ladder system was proposed in [32].

Besides its relevance to ladder compounds, the study of two-chain systems is also important for the study of transport in systems such as metallic carbon nanotubes [33,34] and quantum wires [35–38]. It has also a theoretical interest in itself since the interplay of localization and interaction in dimension higher than one remains poorly understood [39] and coupled quasi-one dimensional system may allow for a controlled study of the effect of increasing space dimensionality on disorder and interaction.

In the present paper, we extend the work of references [22,23] to arbitrary ratio of disorder to interchain

[a] e-mail: orignac@lpt.ens.fr
[b] CNRS-UMR 8549

coupling. A study in the case of spinless fermions revealed an interesting transition from two chain to single chain behavior as disorder strength was increased [40], indicating confinement of fermions by disorder. We shall analyze the two chain system with disorder by bosonization [41–45] and RG (renormalization group) techniques and discuss the different disordered phases that are obtained as well as the confinement phase [46,47]. We use the same techniques as Kawakami and Fujimoto [48], who analyzed the interplay of disorder and Umklapp scattering in the two chain ladder at commensurate filling in the regime in which interchain hopping is dominant [48]. However we examine a different system at incommensurate filling, but allow disorder to become stronger than interchain hopping. Other related work in the ladder considered the effect of forward scattering on the renormalization of disorder [49–51] neglecting the influence of gap openings on localization properties. Such an approximation is restricted to the limit of high temperature or short system, and can be recovered from the general RGE (renormalization group equation) of the present article.

The plan of the paper is as follows. In Section 2, we will recall the derivation of the bosonized Hamiltonian of the system. Then, in Section 3 we will show the RG equations of the system while those of the limit of large interchain hopping is derived in Section 4 to compare with other related work. In Section 5, we will demonstrate several types of spin gapped phases based on the outcome of RG. Finally discussion is given in Section 6.

2 Hamiltonian

The original lattice Hamiltonian of two-chain Hubbard model with disorder reads:

$$H = -t\sum_{i,p,\sigma}(c^{\dagger}_{i,p,\sigma}c_{i+1,p,\sigma} + \text{h.c.}) - t_{\perp}\sum_{i,\sigma}(c^{\dagger}_{i,1,\sigma}c_{i,2,\sigma} + \text{h.c.}) + U\sum_{i,p} n_{i,p,\uparrow}n_{i,p,\downarrow} + \sum_{i,p,\sigma}\epsilon_{i,p}n_{i,p,\sigma}, \quad (1)$$

where $n_{i,p,\sigma} = c^{\dagger}_{i,p,\sigma}c_{i,p,\sigma}$ and $\overline{\epsilon_{i,p}\epsilon_{i',p'}} = W\delta_{i,i'}\delta_{p,p'}$.

We turn to the bonding antibonding band representation:

$$c_{i,0,\sigma} = \frac{c_{i,1,\sigma} + c_{i,2,\sigma}}{\sqrt{2}}, \quad (2)$$

$$c_{i,\pi,\sigma} = \frac{c_{i,1,\sigma} - c_{i,2,\sigma}}{\sqrt{2}}, \quad (3)$$

and use the continuum limit to apply bosonization techniques [6,23,50]. Thus the Hamiltonian can be rewritten as:

$$H = H_{\text{pure}} + H_{\text{impurity}}, \quad (4)$$

$$\begin{aligned} H_{\text{pure}} = {} & \sum_{\substack{\nu=\rho,\sigma\\ r=\pm}}\int\frac{\mathrm{d}x}{2\pi}\left[u_\nu K_{\nu r}(\pi\Pi_{\nu r})^2 + \frac{u_\nu}{K_{\nu r}}(\partial_x\phi_{\nu r})^2\right] \\ & + \frac{2t_\perp}{\pi}\int \mathrm{d}x\partial_x\phi_{\rho-} \\ & + \frac{v_{\text{F}}}{2\pi a^2}\int \mathrm{d}x\,[y_1\cos 2\theta_{\rho-}\cos 2\phi_{\sigma+} \\ & + y_2\cos 2\theta_{\rho-}\cos 2\theta_{\sigma-} \\ & + y_3\cos 2\theta_{\rho-}\cos 2\phi_{\sigma-} + y_4\cos 2\theta_{\rho-}\cos 2\phi_{\rho-} \\ & + y_5\cos 2\phi_{\rho-}\cos 2\phi_{\sigma+} + y_6\cos 2\phi_{\rho-}\cos 2\theta_{\sigma-} \\ & + y_7\cos 2\phi_{\rho-}\cos 2\phi_{\sigma-} + y_8\cos 2\theta_{\sigma-}\cos 2\phi_{\sigma-} \\ & + y_9\cos 2\phi_{\sigma+}\cos 2\phi_{\sigma-} + y_{10}\cos 2\phi_{\sigma+}\cos 2\theta_{\sigma-}], \end{aligned} \quad (5)$$

$$\begin{aligned} H_{\text{impurity}} = {} & \frac{2}{\pi a}\int \mathrm{d}x\,[\eta_a(x) \\ & \times\{\cos(\theta_{\rho-}-\phi_{\rho-})\cos(\theta_{\sigma-}-\phi_{\sigma-}) \\ & + \cos(\theta_{\rho-}+\phi_{\rho-})\cos(\theta_{\sigma-}+\phi_{\sigma-})\} \\ & + \xi_a(x)O_{\text{CDW}^\pi}(x) + \text{h.c.} - a\eta_s(x)\partial_x\phi_{\rho+} \\ & + \xi_s(x)O_{\text{CDW}^0}(x) + \text{h.c.}], \end{aligned} \quad (6)$$

where $O_{\text{CDW}^0}(x)$ ($O_{\text{CDW}^\pi}(x)$) denotes a operator of CDW (charge density wave) with in phase (out of phase) between two chains and is defined by

$$\begin{aligned} O_{\text{CDW}^0}(x) = {} & \mathrm{e}^{\mathrm{i}\phi_{\rho+}}\{\sin\phi_{\rho-}\cos\phi_{\sigma+}\cos\phi_{\sigma-} \\ & -\mathrm{i}\cos\phi_{\rho-}\sin\phi_{\sigma+}\sin\phi_{\sigma-}\}, \end{aligned} \quad (7)$$

$$\begin{aligned} O_{\text{CDW}^\pi}(x) = {} & \mathrm{e}^{\mathrm{i}\phi_{\rho+}}\{\cos\theta_{\rho-}\cos\theta_{\sigma-}\cos\phi_{\sigma+} \\ & +\mathrm{i}\sin\theta_{\rho-}\sin\theta_{\sigma-}\sin\phi_{\sigma+}\}. \end{aligned} \quad (8)$$

The quantity $\Pi_{\nu,r}(x)$ is a variable canonically conjugate to $\phi_{\nu,r}(x)$ and satisfies

$$[\phi_{\nu,r}(x), \Pi_{\nu',r'}(x')] = \mathrm{i}\delta(x-x')\delta_{\nu,\nu'}\delta_{r,r'}, \quad (9)$$

where

$$\theta_{\nu,r}(x) = \pi\int_{-\infty}^{x}\mathrm{d}x'\Pi_{\nu,r}(x'). \quad (10)$$

From bosonization rules, these quantities are written as ($m = 0, \pi$)

$$\frac{c_{n,m,\sigma}}{\sqrt{a}} = \mathrm{e}^{\mathrm{i}k_{\text{F}}x}\frac{\mathrm{e}^{\mathrm{i}(\theta_{m,\sigma}-\phi_{m,\sigma})}}{\sqrt{2\pi a}} + \mathrm{e}^{-\mathrm{i}k_{\text{F}}x}\frac{\mathrm{e}^{\mathrm{i}(\theta_{m,\sigma}+\phi_{m,\sigma})}}{\sqrt{2\pi a}}, \quad (11)$$

$$\phi_{\rho+} = \frac{1}{2}(\phi_{0,\uparrow} + \phi_{0,\downarrow} + \phi_{\pi,\uparrow} + \phi_{\pi,\downarrow}), \quad (12)$$

$$\phi_{\rho-} = \frac{1}{2}(\phi_{0,\uparrow} + \phi_{0,\downarrow} - \phi_{\pi,\uparrow} - \phi_{\pi,\downarrow}), \quad (13)$$

$$\phi_{\sigma+} = \frac{1}{2}(\phi_{0,\uparrow} - \phi_{0,\downarrow} + \phi_{\pi,\uparrow} - \phi_{\pi,\downarrow}), \quad (14)$$

$$\phi_{\sigma-} = \frac{1}{2}(\phi_{0,\uparrow} - \phi_{0,\downarrow} - \phi_{\pi,\uparrow} + \phi_{\pi,\downarrow}), \tag{15}$$

$$\Pi_{\rho+} = \frac{1}{2}(\Pi_{0,\uparrow} + \Pi_{0,\downarrow} + \Pi_{\pi,\uparrow} + \Pi_{\pi,\downarrow}), \tag{16}$$

$$\Pi_{\rho-} = \frac{1}{2}(\Pi_{0,\uparrow} + \Pi_{0,\downarrow} - \Pi_{\pi,\uparrow} - \Pi_{\pi,\downarrow}), \tag{17}$$

$$\Pi_{\sigma+} = \frac{1}{2}(\Pi_{0,\uparrow} - \Pi_{0,\downarrow} + \Pi_{\pi,\uparrow} - \Pi_{\pi,\downarrow}), \tag{18}$$

$$\Pi_{\sigma-} = \frac{1}{2}(\Pi_{0,\uparrow} - \Pi_{0,\downarrow} - \Pi_{\pi,\uparrow} + \Pi_{\pi,\downarrow}). \tag{19}$$

The coupling constants of the bosonized Hamiltonian (4) can be expressed as the function of those of the lattice Hamiltonian (1). They are given by

$$y_1 = y_3 = y_4 = y_9 = y_{10} = -y_5 = -y_6 = -y_8 = \frac{Ua}{\pi v_{\rm F}},$$
$$y_2 = y_7 = 0, \tag{20}$$

and

$$K_{\nu-} = 1, \tag{21}$$
$$u_{\nu-} = v_{\rm F},$$
$$K_{\rho+} = \left(1 + \frac{Ua}{\pi v_{\rm F}}\right)^{-1/2}, \tag{22}$$
$$u_{\rho+} = v_{\rm F}\left(1 + \frac{Ua}{\pi v_{\rm F}}\right)^{1/2}, \tag{23}$$
$$K_{\sigma+} = \left(1 - \frac{Ua}{\pi v_{\rm F}}\right)^{-1/2}, \tag{24}$$
$$u_{\sigma+} = \left(1 - \frac{Ua}{\pi v_{\rm F}}\right)^{1/2}, \tag{25}$$
$$\mathcal{D}_r = \frac{D_r^b a}{\pi v_{\rm F}^2}, \tag{26}$$

where $D_r^f = D_r^b = 2Wa \equiv D$, $\overline{\eta_r(x)\eta_{r'}(x')} = 2D_r^f\delta(x - x')\delta_{r,r'}$ and $\overline{\xi_r(x)\xi_{r'}^*(x')} = 2D_r^b\delta(x - x')\delta_{r,r'}$. $v_{\rm F}$ is the Fermi velocity in the absence of interaction. We note that there is a freedom of sign in choosing the initial condition [54] although the result remains the same. Actually, the initial value of y_1, y_5 and y_{10} in equation (20) has a sign opposite to that of [47], *i.e.*, the correspondence is given by the replacement of $\phi_{\sigma+} \to \phi_{\sigma+} + \pi/2$. We consider only the backward scattering for impurity, which is relevant to the localization.

3 RG equations

The RG equations can be derived from the Hamiltonian (4) using the Operator Product Expansion (OPE) approach [52]. In the RGE, we neglect the velocity differences between the different sectors. To be consistent with such an approximation, we also have to neglect y_4, y_8 in the RGE Failing to do so leads to unphysical results such as a spin gap for $t_\perp = 0$ and no disorder in disagreement with the exact results on the single chain Hubbard model [44]. It is also necessary to expand the RG equations of $K_{\sigma\pm}$ to first order to ensure SU(2) symmetry. The renormalization group equations read:

$$\frac{{\rm d}K_{\rho+}}{{\rm d}l} = -\frac{K_{\rho+}^2}{4}(\mathcal{D}_s + \mathcal{D}_a), \tag{27}$$

$$\frac{{\rm d}K_{\rho-}}{{\rm d}l} = \frac{1}{8}\left[y_1^2 + y_2^2 + y_3^2 + 2\mathcal{D}_a - K_{\rho-}^2\left\{(y_5^2+y_6^2+y_7^2)J_0(4K_{\rho-}\tilde{t}_\perp)+2\mathcal{D}_s\right\}\right], \tag{28}$$

$$\frac{{\rm d}y_{\sigma-}}{{\rm d}l} = \frac{1}{4}\left[y_2^2 + y_6^2 J_0(4K_{\rho-}\tilde{t}_\perp) + y_{10}^2 + 2\mathcal{D}_a - \left\{y_3^2 + y_7^2 J_0(4K_{\rho-}\tilde{t}_\perp) + y_9^2 + 2\mathcal{D}_s\right\}\right], \tag{29}$$

$$\frac{{\rm d}y_{\sigma+}}{{\rm d}l} = -\frac{1}{4}\left[y_1^2 + y_5^2 J_0(4K_{\rho-}\tilde{t}_\perp) + y_9^2 + y_{10}^2 + 2(\mathcal{D}_s + \mathcal{D}_a)\right], \tag{30}$$

$$\frac{{\rm d}y_1}{{\rm d}l} = \left(1 - \frac{1}{K_{\rho-}} - \frac{y_{\sigma+}}{2}\right)y_1 - \frac{1}{2}(y_2 y_{10} + y_3 y_9) - \mathcal{D}_a, \tag{31}$$

$$\frac{{\rm d}y_2}{{\rm d}l} = \left(1 - \frac{1}{K_{\rho-}} + \frac{y_{\sigma-}}{2}\right)y_2 - \frac{1}{2}y_1 y_{10} - \mathcal{D}_a, \tag{32}$$

$$\frac{{\rm d}y_3}{{\rm d}l} = \left(1 - \frac{1}{K_{\rho-}} - \frac{y_{\sigma-}}{2}\right)y_3 - \frac{1}{2}y_1 y_9, \tag{33}$$

$$\frac{{\rm d}y_5}{{\rm d}l} = \left(1 - K_{\rho-} - \frac{y_{\sigma+}}{2}\right)y_5 - \frac{1}{2}(y_7 y_9 + y_6 y_{10}) + \mathcal{D}_s, \tag{34}$$

$$\frac{{\rm d}y_6}{{\rm d}l} = \left(1 - K_{\rho-} + \frac{y_{\sigma-}}{2}\right)y_6 - \frac{1}{2}y_5 y_{10}, \tag{35}$$

$$\frac{{\rm d}y_7}{{\rm d}l} = \left(1 - K_{\rho-} - \frac{y_{\sigma-}}{2}\right)y_7 - \frac{1}{2}y_5 y_9 + \mathcal{D}_s, \tag{36}$$

$$\frac{{\rm d}y_9}{{\rm d}l} = -\frac{1}{2}(y_{\sigma-}y_9 + y_{\sigma+}y_9 + y_1 y_3 + y_5 y_7 J_0(4K_{\rho-}\tilde{t}_\perp)) - \mathcal{D}_s, \tag{37}$$

$$\frac{{\rm d}y_{10}}{{\rm d}l} = -\frac{1}{2}(y_{\sigma+}y_{10} - y_{\sigma-}y_{10} + y_1 y_2 + y_5 y_6 J_0(4K_{\rho-}\tilde{t}_\perp))) - \mathcal{D}_a, \tag{38}$$

$$\frac{{\rm d}\tilde{t}_\perp}{{\rm d}l} = \tilde{t}_\perp - \frac{1}{16}(y_5^2 + y_6^2 + y_7^2)J_1(4K_{\rho-}\tilde{t}_\perp)), \tag{39}$$

$$\frac{{\rm d}\mathcal{D}_a}{{\rm d}l} = \left\{2 - \frac{1}{2}(K_{\rho+} + \frac{1}{K_{\rho-}}) - \frac{1}{4}y_{\sigma+} + \frac{1}{4}y_{\sigma-} - \frac{1}{2}y_1 - \frac{1}{2}y_2 - \frac{1}{2}y_{10}\right\}\mathcal{D}_a, \tag{40}$$

$$\frac{{\rm d}\mathcal{D}_s}{{\rm d}l} = \left\{2 - \frac{1}{2}(K_{\rho+} + K_{\rho-}) - \frac{1}{4}y_{\sigma+} - \frac{1}{4}y_{\sigma-} + \frac{1}{2}y_5 J_0(4K_{\rho-}\tilde{t}_\perp) + \frac{1}{2}y_7 J_0(4K_{\rho-}\tilde{t}_\perp) - \frac{1}{2}y_9\right\}\mathcal{D}_s, \tag{41}$$

where we have introduced $y_{\sigma\pm}$ and $\tilde{t}_\perp$ defined respectively by $K_{\sigma\pm} = 1 + y_{\sigma\pm}/2$ and $\tilde{t}_\perp = \frac{t_\perp a}{\pi v_{\rm F}}$.

In these RG equations, we have neglected the generation of a $4k_{\rm F}$ disorder from $2k_{\rm F}$ disorder since the generation of such term in RG demands special treatment [53]. In the present calculation, we will be finding SC^d and SC^s phases, in which the $2k_{\rm F}$ disorder is regarded as irrelevant. However, based on the study of reference [23] we already know that $4k_{\rm F}$ disorder is always relevant in the SC^d phase and relevant in the SC^s except for $K_{\rho+} > 3/2$. Therefore, in reality these phases of SC^d and SC^s will be replaced by a pinned $4k_{\rm F}$ CDW as discussed in reference [48].

3.1 The limit of $\mathcal{D} = 0$: the pure two-chain ladder

In the limit where $\mathcal{D} = 0$, a simplified form of the RGEs is obtained as:

$$\frac{\mathrm{d}K_{\rho+}}{\mathrm{d}l} = 0 \tag{42}$$

$$\frac{\mathrm{d}K_{\rho-}}{\mathrm{d}l} = \frac{1}{8}\left[y_1^2 + y_2^2 + y_3^2 - K_{\rho-}^2\left\{(y_5^2 + y_6^2 + y_7^2)J_0(4K_{\rho-}\tilde{t}_\perp)\right\}\right], \tag{43}$$

$$\frac{\mathrm{d}y_{\sigma-}}{\mathrm{d}l} = \frac{1}{4}\left[y_2^2 + y_6^2 J_0(4K_{\rho-}\tilde{t}_\perp) + y_{10}^2 - \left\{y_3^2 + y_7^2 J_0(4K_{\rho-}\tilde{t}_\perp) + y_9^2\right\}\right], \tag{44}$$

$$\frac{\mathrm{d}y_{\sigma+}}{\mathrm{d}l} = -\frac{1}{4}\left[y_1^2 + y_5^2 J_0(4K_{\rho-}\tilde{t}_\perp) + y_9^2 + y_{10}^2\right], \tag{45}$$

$$\frac{\mathrm{d}y_1}{\mathrm{d}l} = \left(1 - \frac{1}{K_{\rho-}} - \frac{y_{\sigma+}}{2}\right) y_1 - \frac{1}{2}(y_2 y_{10} + y_3 y_9), \tag{46}$$

$$\frac{\mathrm{d}y_2}{\mathrm{d}l} = \left(1 - \frac{1}{K_{\rho-}} + \frac{y_{\sigma-}}{2}\right) y_2 - \frac{1}{2} y_1 y_{10}, \tag{47}$$

$$\frac{\mathrm{d}y_3}{\mathrm{d}l} = \left(1 - \frac{1}{K_{\rho-}} - \frac{y_{\sigma-}}{2}\right) y_3 - \frac{1}{2} y_1 y_9, \tag{48}$$

$$\frac{\mathrm{d}y_5}{\mathrm{d}l} = \left(1 - K_{\rho-} - \frac{y_{\sigma+}}{2}\right) y_5 - \frac{1}{2}(y_7 y_9 + y_6 y_{10}), \tag{49}$$

$$\frac{\mathrm{d}y_6}{\mathrm{d}l} = \left(1 - K_{\rho-} + \frac{y_{\sigma-}}{2}\right) y_6 - \frac{1}{2} y_5 y_{10}, \tag{50}$$

$$\frac{\mathrm{d}y_7}{\mathrm{d}l} = \left(1 - K_{\rho-} - \frac{y_{\sigma-}}{2}\right) y_7 - \frac{1}{2} y_5 y_9, \tag{51}$$

$$\frac{\mathrm{d}y_9}{\mathrm{d}l} = -\frac{1}{2}(y_{\sigma-} y_9 + y_{\sigma+} y_9 + y_1 y_3 + y_5 y_7 J_0(4K_{\rho-}\tilde{t}_\perp)), \tag{52}$$

$$\frac{\mathrm{d}y_{10}}{\mathrm{d}l} = -\frac{1}{2}(y_{\sigma+} y_{10} - y_{\sigma-} y_{10} + y_1 y_2 + y_5 y_6 J_0(4K_{\rho-}\tilde{t}_\perp))), \tag{53}$$

$$\frac{\mathrm{d}\tilde{t}_\perp}{\mathrm{d}l} = \tilde{t}_\perp - \frac{1}{16}(y_5^2 + y_6^2 + y_7^2) J_1(4K_{\rho-}\tilde{t}_\perp)). \tag{54}$$

These equations are identical to those previously derived in [47]. Taking the limit of $t_\perp \to +\infty$, which is the limit of the two chain system, these equations are further simplified [11,10]:

$$\frac{\mathrm{d}K_{\rho-}}{\mathrm{d}l} = \frac{1}{8}(y_1^2 + y_2^2 + y_3^2), \tag{55}$$

$$\frac{\mathrm{d}y_{\sigma-}}{\mathrm{d}l} = \frac{1}{4}\left[y_2^2 + y_{10}^2 - (y_3^2 + y_9^2)\right], \tag{56}$$

$$\frac{\mathrm{d}y_{\sigma+}}{\mathrm{d}l} = -\frac{1}{4}\left[y_1^2 + y_9^2 + y_{10}^2\right], \tag{57}$$

$$\frac{\mathrm{d}y_1}{\mathrm{d}l} = \left(1 - \frac{1}{K_{\rho-}} - \frac{y_{\sigma+}}{2}\right) y_1 - \frac{1}{2}(y_2 y_{10} + y_3 y_9), \tag{58}$$

$$\frac{\mathrm{d}y_2}{\mathrm{d}l} = \left(1 - \frac{1}{K_{\rho-}} + \frac{y_{\sigma-}}{2}\right) y_2 - \frac{1}{2} y_1 y_{10}, \tag{59}$$

$$\frac{\mathrm{d}y_3}{\mathrm{d}l} = \left(1 - \frac{1}{K_{\rho-}} - \frac{y_{\sigma-}}{2}\right) y_3 - \frac{1}{2} y_1 y_9, \tag{60}$$

$$\frac{\mathrm{d}y_9}{\mathrm{d}l} = -\frac{1}{2}(y_{\sigma-} y_9 + y_{\sigma+} y_9 + y_1 y_3), \tag{61}$$

$$\frac{\mathrm{d}y_{10}}{\mathrm{d}l} = -\frac{1}{2}(y_{\sigma+} y_{10} - y_{\sigma-} y_{10} + y_1 y_2). \tag{62}$$

Obviously, one has: $K_{\rho-} \to +\infty, y_{\sigma+} \to -\infty$. Moreover, it is easily seen from initial conditions that originally $|y_2| < |y_3|$ and $|y_9| = |y_{10}|$, resulting in $\frac{\mathrm{d}y_{\sigma-}}{\mathrm{d}l} < 0$. Thus, for small l, one should have $y_{\sigma-} < 0$. This in turn makes y_2, y_{10} less relevant and results in both $\frac{\mathrm{d}y_{\sigma-}}{\mathrm{d}l}$ and $y_{\sigma-}$ becoming more negative. As a result, one finds $y_{\sigma-} \to -\infty$. Thus $\theta_{\rho-}$ and $\phi_{\sigma\pm}$ become locked in the ladder system. Further analysis of these RGE shows that there are two possible fixed points [54,6] depending on the sign of U as represented on Table 1. The fixed point for $U > 0$ correspond to the formation of d-wave superconductivity, whereas the one for $U < 0$ corresponds to the formation of s-wave superconductivity.

Table 1. The two possible fixed points in a two-chain Hubbard ladder.

$U > 0$	$\langle\theta_{\rho-}\rangle = 0$	$\langle\phi_{\sigma-}\rangle = \frac{\pi}{2}$	$\langle\phi_{\sigma+}\rangle = \frac{\pi}{2}$
$U < 0$	$\langle\theta_{\rho-}\rangle = 0$	$\langle\phi_{\sigma-}\rangle = 0$	$\langle\phi_{\sigma+}\rangle = 0$

3.2 The case $t_\perp = 0$: single chain limit

This case corresponds to two decoupled disordered Hubbard chains and has been analyzed in details in reference [21]. A crucial test of the validity of our RG equations is whether we can recover the RG equations of reference [21] by putting $t_\perp = 0$ in equations (27–41). For $t_\perp = 0$, it is straightforward to show that the solution of the RG equations (27–41) satisfies:

$$\mathcal{D}_s(l) = \mathcal{D}_a(l) = \mathcal{D}(l), \tag{63}$$

$$y_6(l) = -y_3(l), \tag{64}$$

$$y_7(l) = -y_2(l), \tag{65}$$

$$K_{\rho-}(l) = K_{\sigma-}(l) = 1, \tag{66}$$

$$y_{\sigma+}(l) = y_1(l) = y_9(l) = y_{10}(l) = -y_5(l) = y_2(l) + y_3(l) = y(l). \tag{67}$$

As a result, the RG equations (27–41) are reduced to the following equivalent set:

$$\frac{\mathrm{d}K_{\rho+}}{\mathrm{d}l} = -\frac{K_{\rho+}^2}{2}\mathcal{D}, \tag{68}$$

$$\frac{\mathrm{d}y}{\mathrm{d}l} = -y^2 - \mathcal{D}, \tag{69}$$

$$\frac{\mathrm{d}y_2}{\mathrm{d}l} = -\frac{y^2}{2} - \mathcal{D}, \tag{70}$$

$$\frac{\mathrm{d}y_3}{\mathrm{d}l} = -\frac{y^2}{2}, \tag{71}$$

$$\frac{\mathrm{d}\mathcal{D}}{\mathrm{d}l} = \left(\frac{3}{2} - \frac{K_{\rho+}}{2} - \frac{5}{4}y - \frac{1}{2}y_2\right)\mathcal{D}. \tag{72}$$

Using the expansion: $K_{\rho+} = 1 + y_{\rho+}/2$, we rewrite the RG equation for $K_{\rho+}$ in the form:

$$\frac{\mathrm{d}y_{\rho+}}{\mathrm{d}l} = -\mathcal{D}, \tag{73}$$

with $y_{\rho+}(0) = -y(0)$. It is then easily seen that $y_2(l) = (y_{\rho+}(l) + y(l))/2$, for all l. This allows to rewrite the RGE for $\mathcal{D}$ as:

$$\frac{1}{\mathcal{D}}\frac{\mathrm{d}\mathcal{D}}{\mathrm{d}l} = 2 - K_{\rho+} - \frac{3}{2}y_{\sigma+}. \tag{74}$$

The RGE equations are thus reduced to those of the single chain case (see Eq. (3.12) in Ref. [21]). Then, our RG equations have the correct limit of $t_\perp = 0$. Obviously, for $\mathcal{D} = 0$, we recover the RGEs that can be applied to a single chain system. In particular, we can easily check that the system develops a spin gap for $U < 0$ but remains gapless for $U > 0$. Thus, we see that the RGEs (27–41) correctly capture the limit of a single chain system.

4 The limit $t_\perp \to \infty$: two chain regime

In this section, we consider the limit $t_\perp \to \infty$ of the equations (27–41) in order to make contact with the work of references [48,51,49,50]. In the limit $t_\perp \to \infty$, the Bessel functions are negligible, so that equations (27–41) are reduced to:

$$\frac{\mathrm{d}K_{\rho+}}{\mathrm{d}l} = -\frac{K_{\rho+}^2}{4}(\mathcal{D}_s + \mathcal{D}_a), \tag{75}$$

$$\frac{\mathrm{d}K_{\rho-}}{\mathrm{d}l} = \frac{1}{8}\left[y_1^2 + y_2^2 + y_3^2 + 2\mathcal{D}_a - 2K_{\rho-}^2\mathcal{D}_s\right], \tag{76}$$

$$\frac{\mathrm{d}y_{\sigma-}}{\mathrm{d}l} = \frac{1}{4}\left[y_2^2 + y_{10}^2 + 2\mathcal{D}_a - \left\{y_3^2 + y_9^2 + 2\mathcal{D}_s\right\}\right], \tag{77}$$

$$\frac{\mathrm{d}y_{\sigma+}}{\mathrm{d}l} = -\frac{1}{4}\left[y_1^2 + y_9^2 + y_{10}^2 + 2(\mathcal{D}_s + \mathcal{D}_a)\right], \tag{78}$$

$$\frac{\mathrm{d}y_1}{\mathrm{d}l} = \left(1 - \frac{1}{K_{\rho-}} - \frac{y_{\sigma+}}{2}\right)y_1 - \frac{1}{2}(y_2 y_{10} + y_3 y_9) - \mathcal{D}_a, \tag{79}$$

$$\frac{\mathrm{d}y_2}{\mathrm{d}l} = \left(1 - \frac{1}{K_{\rho-}} + \frac{y_{\sigma-}}{2}\right)y_2 - \frac{1}{2}y_1 y_{10} - \mathcal{D}_a, \tag{80}$$

$$\frac{\mathrm{d}y_3}{\mathrm{d}l} = \left(1 - \frac{1}{K_{\rho-}} - \frac{y_{\sigma-}}{2}\right)y_3 - \frac{1}{2}y_1 y_9, \tag{81}$$

$$\frac{\mathrm{d}y_9}{\mathrm{d}l} = -\frac{1}{2}(y_{\sigma-}y_9 + y_{\sigma+}y_9 + y_1 y_3) - \mathcal{D}_s, \tag{82}$$

$$\frac{\mathrm{d}y_{10}}{\mathrm{d}l} = -\frac{1}{2}(y_{\sigma+}y_{10} - y_{\sigma-}y_{10} + y_1 y_2) - \mathcal{D}_a, \tag{83}$$

$$\frac{\mathrm{d}\mathcal{D}_a}{\mathrm{d}l} = \left\{2 - \frac{1}{2}(K_{\rho+} + \frac{1}{K_{\rho-}}) - \frac{1}{4}y_{\sigma+} + \frac{1}{4}y_{\sigma-} - \frac{1}{2}y_1 - \frac{1}{2}y_2 - \frac{1}{2}y_{10}\right\}\mathcal{D}_a, \tag{84}$$

$$\frac{\mathrm{d}\mathcal{D}_s}{\mathrm{d}l} = \left\{2 - \frac{1}{2}(K_{\rho+} + K_{\rho-}) - \frac{1}{4}y_{\sigma+} - \frac{1}{4}y_{\sigma-} - \frac{1}{2}y_9\right\}\mathcal{D}_s, \tag{85}$$

Let us compare our equations with those in [50]. Equations (11, 12, 14, 15) in reference [50] correspond respectively to equations (84, 82, 83) and (79) in the present paper. However, in equations (12, 14) and (15) of [50] we do not find terms arising from coupling between interactions, which give rise to the same order. More importantly, equation (85) is in disagreement with equation (10) in reference [50]. The reason is that in reference [50], the y_5 term was kept although it should drop from the Hamiltonian when $t_\perp$ becomes sufficiently large. The correct initial RG equations for weak disorder and large $t_\perp$ thus read:

$$\frac{\mathrm{d}\mathcal{D}_a}{\mathrm{d}l} = \left(1 - \frac{Ua}{\pi v_\mathrm{F}}\right)\mathcal{D}_a \tag{86}$$

$$\frac{\mathrm{d}\mathcal{D}_s}{\mathrm{d}l} = \left(1 - \frac{Ua}{2\pi v_\mathrm{F}}\right)\mathcal{D}_s. \tag{87}$$

These equations imply that antisymmetric disorder is more relevant than symmetric disorder in the case of attractive interaction and less relevant for repulsive interactions. Such result can be understood in the following way: for repulsive interactions, the system tends to form interchain Cooper pairs and thus to have a repartition of charges that is symmetric between the two ladders. This makes the system less sensitive to antisymmetric disorder. For attractive interactions, the system prefers to form intrachain Cooper pairs. If electrons of the Cooper pair can tunnel on the opposite chain in a virtual process, the energy of the Cooper pair is lowered. This results in interchain repulsion of the pairs and thus antisymmetric CDW fluctuations. This mechanism obviously makes antisymmetric disorder a more relevant perturbation.

Comparing with reference [48], we have similar equations once we put the Umklapp process of reference [48] equal to zero. However, an important difference between the present paper and [48] is that in [48] a random $t_\perp$ term is also included in the Hamiltonian. This random $t_\perp$ can result in closure of the transverse charge gap and thus can lead to a rather different physics from the one discussed here, closer to the one considered in [49–51]. We will

Table 2. The fixed points of the disordered two-chain Hubbard ladder.

I	$\langle\theta_{\rho-}\rangle = 0$	$\langle\phi_{\sigma-}\rangle = \frac{\pi}{2}$	$\langle\phi_{\sigma+}\rangle = \frac{\pi}{2}$	$t_\perp \to \infty$
IIa	$K_{\rho-} \simeq 1$	$K_{\sigma-} \simeq 1$	$\langle\phi_{\sigma+}\rangle = 0$	$t_\perp \to 0$
IIb	$\langle\theta_{\rho-}\rangle = 0$	$\langle\phi_{\sigma-}\rangle = 0$	$\langle\phi_{\sigma+}\rangle = 0$	$t_\perp \to \infty$
III	$\langle\theta_{\rho-}\rangle = 0$	$\langle\theta_{\sigma-}\rangle = 0$	$\langle\phi_{\sigma+}\rangle = 0$	$t_\perp \to \infty$
IV	$K_{\rho-} \simeq 1$	$K_{\sigma-} \simeq 1$	$\langle\phi_{\sigma+}\rangle = 0$	$t_\perp \to 0$

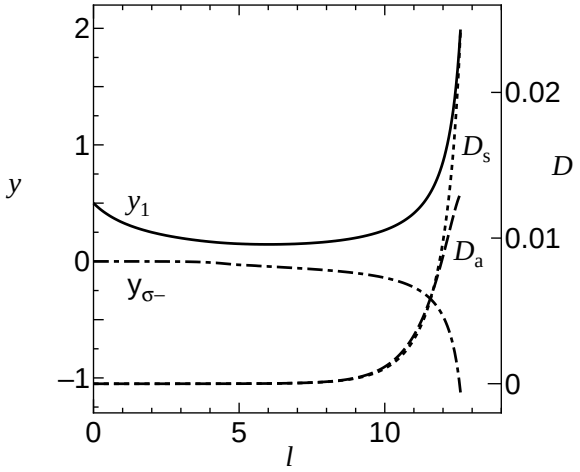

Fig. 1. RG flow as a function of l for the SCd phase with $Ua/\pi v_F = 0.5$, $t_\perp = 10^{-2}$ and $D = 10^{-7}$ where the left axis is for y_1 and $y_{\sigma-}$ and the right axis is for D_a (dashed curve) and D_s (dotted curve).

compare in more details our results and those of [48] in the next section.

5 Results

From RG equations (27–41), we can distinguish four different phases where the corresponding fixed points are shown on Table 2 (explained below).

5.1 SCd Phase

For large repulsive interaction and small disorder, we obtain the SCd phase, where strong coupling in interaction is reached before strong coupling in disorder. The resulting flow of coupling constants is represented in Figure 1. The ground state has $\langle\theta_{\rho-}\rangle = 0$, $\langle\phi_{\sigma-}\rangle = \langle\phi_{\sigma+}\rangle = \frac{\pi}{2}$ (I in Tab. 2). This phase to the approximation of RG is a metallic phase. It has been discussed in [48] as case A. However, including coupling to $4k_F$ disorder, it is possible to show that such a phase is in fact localized [22,23,48] due to pinning of $4k_F$ CDW fluctuations by disorder [22,23]. We can see that in this phase, D_s is more relevant than D_a which is consistent with equations (86–87). For stronger interaction, this behavior can also be understood from equations (7–8). Replacing $\theta_{\rho-}, \phi_{\sigma\pm}$ by their expectation values in these equations, we obtain $O_{\mathrm{CDW}^0} \sim \mathrm{e}^{\mathrm{i}\phi_{\rho+}} \cos\phi_{\rho-}$ and $O_{\mathrm{CDW}^\pi} \sim \mathrm{e}^{\mathrm{i}\phi_{\rho+}}(\cos\theta_{\sigma-}\cos\phi_{\sigma+} + \mathrm{i}\sin\theta_{\rho-}\sin\theta_{\sigma-})$ where we have kept only the operators with power-law or exponential decay. Clearly, O_{CDW^π} contains more disordered operators with exponential decay than O_{CDW^0}. As a result, CDW^0 are dominating over the CDW^π in the SCd phase, in agreement with the picture of interchain pairing. This also implies that the random potential that couples to O_{CDW^0} is more relevant than the one that coupled to O_{CDW^π} even deep in the SCd phase.

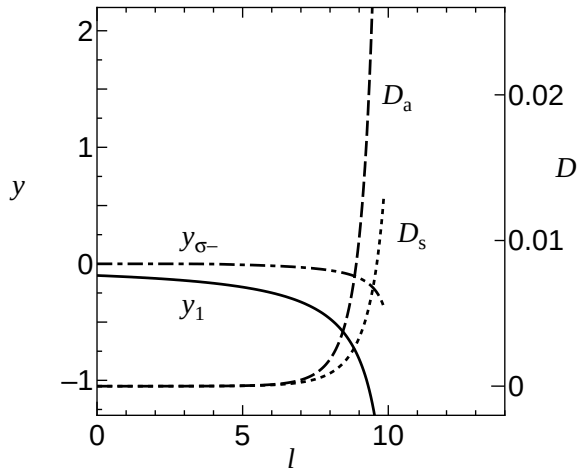

Fig. 2. RG flow as a function of l for the SCs phase with $Ua/\pi v_F = -0.1$, $t_\perp = 10^{-2}$ and $D = 10^{-7}$ where the notations are the same as Figure 1.

5.2 SCs phase

For interaction being moderately attractive and disorder being small, we obtain the phase where strong coupling in interaction is reached before strong coupling in disorder. The resulting flow of coupling constants is represented in Figure 2. In this case, the ground state has $\langle\theta_{\rho-}\rangle = \langle\phi_{\sigma-}\rangle = \langle\phi_{\sigma+}\rangle = 0$ (IIb in Tab. 2). Similarly to the SCd phase, the SCs phase is localized by disorder due to the presence of subdominant $4k_F$ fluctuations [22,23]. However, for attractive enough interactions [22,23] the $4k_F$ CDW can be depinned by quantum fluctuations in contrast with the SCd phase. It can be seen that in the SCs phase, D_a is increasing faster than D_s in agreement with equations (86–87). The persistence of this behavior even when the spin gap is well formed can be understood by the same arguments as in 5.1. Comparing equations (7) and (8). In equation (8), only the operator $\cos\theta_{\sigma-}$ has exponentially decaying correlation, whereas in equation (7) the three operators $\cos\phi_{\rho-}$, $\sin\phi_{\sigma-}$ and $\sin\phi_{\sigma+}$ are disordered with exponentially decaying correlations. As a result, the CDW^0 have a much faster exponential decay than the CDW^π fluctuations inside the SCs phase. In turn, this makes D_s much less relevant than D_a. Physically, this can be understood by noting that attractive interactions form Cooper pair inside a single chain, leading to subdominant CDW^π fluctuations whose transverse charge fluctuation is compatible with that of SCs fluctuations.

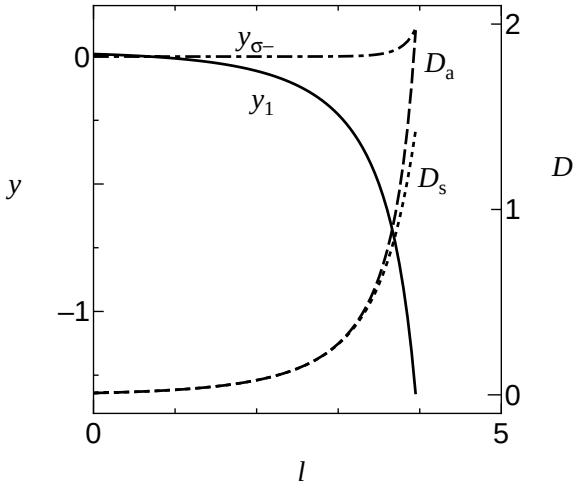

Fig. 3. RG flow as a function of l for the the PCDW phase with $Ua/\pi v_F = 0.01$, $t_\perp = 10^{-2}$ and $D = 10^{-3}$ where the notations are the same as Figure 1.

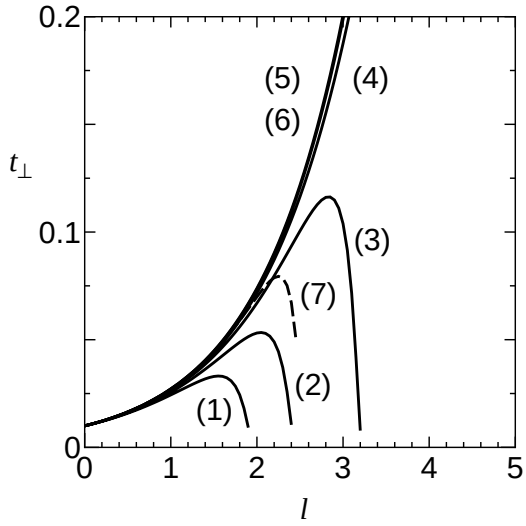

Fig. 4. RG flow of $t_\perp$ showing both confinement (irrelevant $t_\perp$) and deconfinement (relevant $t_\perp$) with $Ua/\pi v_F = -0.5(1)$, $-0.4(2)$, $-0.3(3)$, $-0.2(4)$, $-0.1(5)$ and $0(6)$ where $t_\perp = 10^{-2}$ and $D = 10^{-3}$. The curve (7) also shows the confinement for $Ua/\pi v_F = 0.1$, $t_\perp = 10^{-2}$ and $D = 10^{-1}$.

5.3 PCDW$^\pi$ phase

For intermediate disorder, we obtain the PCDW$^\pi$ phase where strong coupling in the RG equations is obtained for disorder first. The flow of the coupling constants is represented in Figure 3. In this phase, one finds that D_a is diverging faster than D_s. This corresponds to the long range ordering with $\langle\theta_{\rho-}\rangle = \langle\phi_{\sigma+}\rangle = \langle\theta_{\sigma-}\rangle = 0$ (III in Tab. 2). This phase is the pinned CDW$^\pi$ of reference [23] and has also been discussed within a RG approach in [48]. We note that such a phase appears only for disorder strong enough to compete with interaction (*i.e.*, not in the limit of infinitesimal disorder) for the present model. The presence of such phase in the ladder system can have important consequences for transport properties since pinning properties of the CDW$^\pi$ are very different from the $4k_F$ CDW.

5.4 Confinement

If strong coupling in disorder is reached before $\tilde{t}_\perp(l) = 1$, there is a possibility of confinement of carriers in the transverse direction corresponding to the irrelevance of $\tilde{t}_\perp$ [46,47] (IV in Tab. 2). This is represented in Figure 4 (curve (7)). Note that on the figures $t_\perp$ stands for $\tilde{t}_\perp$. This confinement can be understood as the formation of a localized state at an energy scale higher than $t_\perp$. This time, a spin gap is formed at an energy scale higher than $t_\perp$. As a result, we have to distinguish two types of pinned $2k_F$ CDWs. One is the pinned $2k_F$ CDW$^\pi$ of the two chain system (III in Tab. 2), and the second one is the combination of two pinned $2k_F$ CDW in each chain with irrelevant interchain hopping (IV in Tab. 2). In the first case, there is a definite phase relation between the CDW in chain 1 and the CDW in chain 2, while in the second case, such relation is less definite. Such regime could not be obtained with the approximations used in [48] or [23] which are valid only when $\tilde{t}_\perp$ is relevant. Further, we note that confinement can also result from the presence of an attractive interaction in the absence of disorder as seen curves (1, 2) and (3) in Figure 4) (IIa in Tab. 2).

Here the difference in the disordered state between IIa and IV is examined besides the mechanism for confinement. In the region IIa of Figure 5, a Josephson coupling is present and dominates the low energy properties. The physics of this region can be understood by describing the Cooper pair as hard core bosons. The problem is reduced to a disordered bosonic ladder with interchain hopping considered in reference [55]. Thus it is found that the phase in region IIa is a pinned $4k_F$ CDW. In region IV, the localization effects are stronger than the Josephson coupling, leading to two independently pinned $2k_F$ CDWs.

5.5 Criterion for transitions between the different phases

We examine boundaries between several types of phases, which are shown in Figure 5.

5.5.1 Confinement transition

A criterion for disorder confinement can be obtained by comparing the length scale $l_{\rm loc.}$ ($\mathcal{D}(l_{\rm loc.}) = 1$) with the length scale $l_{\rm 2ch.}$ ($t_\perp(l_{\rm 2ch.}) = 1$). Clearly, if $l_{\rm loc.} < l_{\rm 2ch.}$ the system is localized before entering into the two-chain regime and thus the ground state will be formed of two chains pinned on their own disorder. For weak interactions, this criterion corresponds to $\mathcal{D}(0) > t_\perp(0)$. As can be seen in Figure 6, it gives the correct boundary between the pinned $2k_F$ CDW$^\pi$ (phase (III)) and the independently pinned $2k_F$ CDWs (phase (IV)). For stronger interactions,

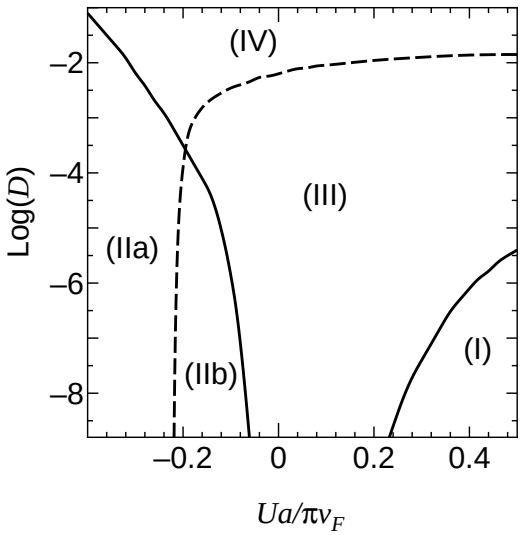

Fig. 5. Phase diagram in the $(\log(\mathcal{D}), U)$ plane for a fixed $t_\perp = 10^{-2}$. The respective phases denote the SCd state (region (I)), the confined SCs state (region (IIa)), the SCs state (region (IIb)) the pinned CDW$^\pi$ state (region (III)) and the pinned CDW$^\pi$ state with confinement (region (IV)).

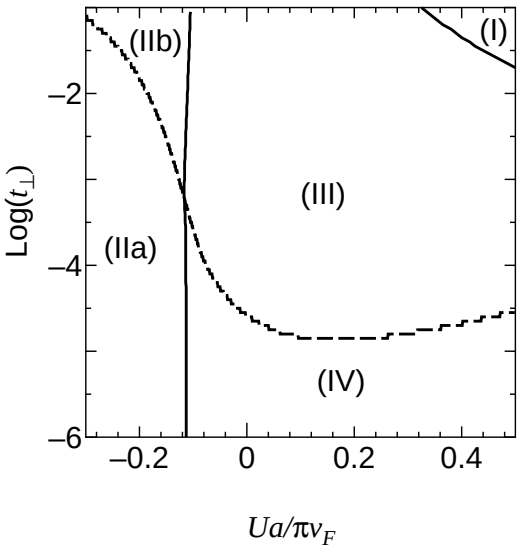

Fig. 6. Phase diagram in the $(t_\perp, U)$ plane for a fixed $D = 10^{-5}$ where the notations are the same as Figure 5.

the criterion for confinement is $E_{\rm loc.} = (v_{\rm F}/a)\mathrm{e}^{-l_{\rm loc.}} = t_\perp$. Since the pinning energy is enhanced in the presence of interactions, this implies that interactions enhance confinements effects as can be seen in Figure 6. In the case of confinement by intrachain interactions one has to compare the scale at which $y(l) = -\infty$ (for $\mathcal{D} = 0$) to the scale at which $\tilde{t}_\perp(l) \sim 1$. Since we have:

$$y(l) = \frac{y(0)}{1 + y(0)l}, \tag{88}$$

we find that confinement occurs when:

$$y(0) = \frac{1}{\ln(\tilde{t}_\perp(0))}\cdot \tag{89}$$

For $\tilde{t}_\perp = 10^{-2}$, this gives confinement when $Ua/\pi v_{\rm F} = -0.22$, which is the correct value for Figure 5 when $\mathcal{D} < 10^{-8}$.

In Figure 5, we see that the two confinement regimes merge to give rise to a single confined phase. An important question is whether the transition between the confined and the deconfined phase is a true phase transition (*i.e.* whether one can find an order parameter for the confined or deconfined phase) or if it is only a crossover. In the case of a commensurate potential (at half-filling), it is well known [47,56,57] that no order parameter exists than can distinguish the confined from the deconfined phase. Thus, we do not expect to see a true transition in the disordered phase. Instead, we expect a progressive loss of phase coherence between the two CDWs in chain 1 and 2.

5.5.2 Transition between PCDW$^\pi$ and SC phases

This transition is obtained in the deconfined regime. A criterion for this transition can be obtained by comparing the $2k_{\rm F}$ CDW pinning energy with the gap in $\sigma-$ sector. When the pinning energy is above the gap, the system gains more energy by being in the PCDW phase. The transverse gap in $\sigma-$ is obtained by applying single chain RG for $\tilde{t}_\perp \mathrm{e}^l \ll 1$ and two chain RG for $\tilde{t}_\perp \mathrm{e}^l \gg 1$. Comparing the transverse gap with the pinning energy leads to a good agreement with the phase boundary between (I) and (III).

5.6 Global phase diagram

The global phase diagram is shown in Figure 5 with the fixed $t_\perp = 10^{-2}$. Based on the criterion in the previous subsection, the boundary between pinned CDW phase (region (III)) and superconducting phases (region (I) or region (IIb)) is given by

$$y_{\sigma-}(l_{\rm loc.}) = 0. \tag{90}$$

The quantity $l_{loc.}$ is the scale at which one of the coupling constants of disorder is equal to one. This is also understood from Figures 1, 2, and 3 where the fixed point of $y_{\sigma-}$ is given by $-\infty$ for regions (I) and (IIb) and ∞ for regions (III). In the confined region, the corresponding boundary is given by $y_{\sigma-}(\infty) = 0$. With increasing D, the pinned CDW region is enlarged. The region for SCs state is much larger than that for SCd state since the spin gap exists even for the single chain. The boundary between region (I) and (III) is also obtained from the condition $y_1(\infty) = 0$ since the fixed point for y_1 is given by ∞ for region (I) and $-\infty$ for region (III). The boundary between (III) and (IIb) (or between (IV) and (IIa)) is also given by $y_2(\infty)/y_3(\infty) = 1$ since $y_2(\infty)/y_3(\infty) > 1 (< 1)$ for region(III) and (IV) (region (IIb) and (IIa)). The boundary between the confined and deconfined phase is given by the condition

$$\tilde{t}_\perp(l_{\rm c}) = 1. \tag{91}$$

The quantity l_c denotes a value at which t_l takes a maximum. The boundary between confinement and deconfinement in the pinned CDW region moves continuously to that in th SCs state. The former is determined by disorder while the latter is determined by attractive interaction. Such a continuous variation of the boundary indicates a fact that the confinement occurs by the combined effect of interchain hopping, intrachain interaction and disorder.

Another global phase diagram is shown in Figure 6 in the $(t_\perp, U)$ plane with a fixed $D = 10^{-5}$ where the notations are the same as Figure 5. The effect of interchain hopping on confinement is opposite to that of disorder in Figure 5. The $t_\perp$ dependence on the boundary between (IV) and (IIa) ((III) and (IIb)) is small while it is noticeable for the boundary between (III) and (IV) ((III) and (I)).

6 Discussion

We have examined the effect of interchain hopping on disordered two-coupled chains using RG equations that enable us to describe the crossover from the single chain to two chain regime. Using the RG equations, we have shown that a $2k_F$ CDW$^\pi$ could be obtained when disorder was strong enough compared to interaction.

In the case of two chains of spinless fermions [40], it is known that for repulsive interactions there is a strong reinforcement of Anderson localization, but complete delocalization for attractive interactions. By contrast, in the case of spinful fermions, the localization-delocalization transition is known to be obtained only for $K_{\rho+} > 3/2$ *i.e.* large attractive interaction strength [23]. Moreover, in the case of repulsive interactions, in contrast with the spinless case, there is no enhancement of localization for infinitesimal disorder [23] in the spinful system. This behavior is due to the fact that both for repulsive and attractive interactions, the localized phase in the presence of infinitesimal disorder is a pinned $4k_F$ CDW. Our RG study shows that when disorder becomes stronger (see Fig. 5) or interchain hopping becomes weaker (see Fig. 6), a $2k_F$ pinned CDW$^\pi$ can be induced in the place of the $4k_F$ CDW. This pinned CDW$^\pi$ has a much shorter localization length than the pinned $4k_F$ CDW. Interestingly, the domain of existence of the PCDW$^\pi$ is larger for repulsive interactions. Thus, for weak but not infinitesimal disorder, localization will be reinforced by repulsive interactions. A similar effect is also obtained by reducing $t_\perp$. This results from the renormalization of interactions in the $\sigma-$ sector by disorder, and could not be obtained within the infinitesimal disorder limit of [23]. Such behavior is represented in Figure 7 where the localization energy $E_{\rm loc.} = \frac{v_F}{\xi_{\rm loc.}}$ and the gap energy $E_{\rm gap} = \frac{v_F}{\xi_{\rm gap}}$ ($\xi_{\rm loc.} = a e^{l_{\rm loc.}}$ and $\xi_{\rm gap} = a e^{l_{\rm gap}}$ being respectively the lengthscale at which disorder or interaction become of order one) are represented a a function of $\tilde{t}_\perp$ for fixed disorder and interaction. A slight enhancement of the pinning energy can be observed for $\tilde{t}_\perp$ large enough to deconfine but not strong enough to make the gaps robust to disorder.

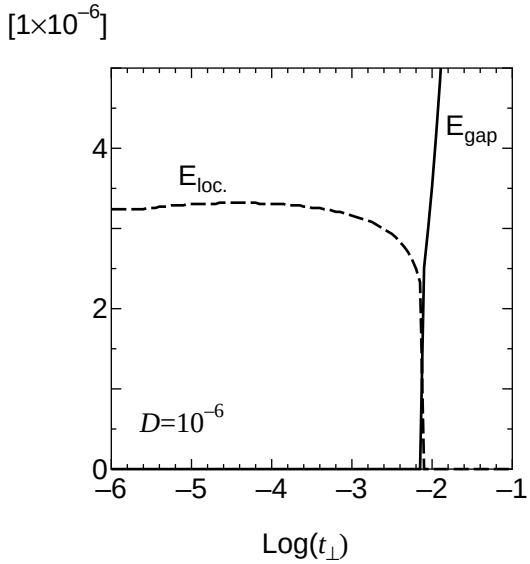

Fig. 7. Behavior of $2k_F$ pinning energy (inverse of localization length) and gap energy as a function of interchain hopping for $y = 0.5$ and $\mathcal{D} = 10^{-6}$. For a given value of $\tilde{t}_\perp$ only the largest of the two energies is represented. We note that for small interchain hopping, there is a small *reinforcement* of localization with respect to the single chain limit. The origin of this reinforcement is the development of $2k_F$ CDW$^\pi$ fluctuations in the system. With stronger interchain hopping, delocalization effects become apparent. Finally, when the interchain spin gap becomes larger than the $2k_F$ pinning energy, the system develops a $4k_F$ pinned CDW with a much smaller pinning energy.

Let us now turn to the question of the crossover from single chain to two chain behavior. In the limit of $\tilde{t}_\perp = 0$ *i.e.* the single chain fermion system, it has been known for some time [58] that the localization length was $\xi_{\rm loc.} \sim (1/D)^{1/(3-K_\rho)}$ for attractive interactions, but $\xi_{\rm loc.} \sim (1/D)^{1/(2-K_\rho)}$ for repulsive interactions, leading to a reinforcement of localization by attractive interactions. This reinforcement of localization results in a maximum of localization length in the vicinity of the noninteracting point. For large $\tilde{t}_\perp$ and infinitesimal disorder, it has been shown in [23] that the localization length was $\xi_{\rm loc.} \sim (1/D)^{2/(3-2K_{\rho+})}$ so that the reinforcement of localization by attractive interactions disappeared. In the present case of intermediate $\tilde{t}_\perp$ and non-infinitesimal disorder, the behavior of the localization length deduced from the RG is richer. For small interaction strength, disorder is strong enough to prevent the formation of SCs or SCd phase in the system, and the behavior of localization length is essentially one dimensional, leading to a maximum of localization length in the vicinity of the noninteracting point. For stronger interactions, the SCs and SCd phases can develop, leading to a strong enhancement of localization length caused by the weaker pinning of $4k_F$ CDWs compared to $2k_F$ CDWs. This result in the presence of two minimums of the localization length as a function of interaction. The corresponding behavior of the pinning energy $E_{\rm loc.} = v_F/\xi_{\rm loc.}$ in the case of $\mathcal{D} = 10^{-5}$ and $Ua/(\pi v_F) = 0.5$ is represented in Figure 8. Interestingly,

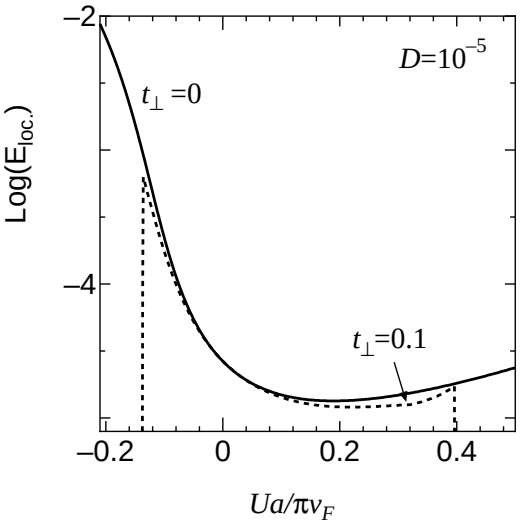

Fig. 8. The behavior of the pinning energy (inverse localization length) a a function of interaction strength for $D = 10^{-5}$ and $t_\perp = 0$ (single chain case, solid line) and $t_\perp = 0.1$ (two chain case, dotted line). For weak interaction, the pinning energy is the same for both systems. This corresponds to the confinement regime. For stronger interaction, the two chain system is always less localized than its single chain counterpart. Thus, a large enough $t_\perp$ always induces delocalization. For an even stronger interaction, the two chain system goes into the pinned $4k_F$ CDW phase with a much longer pinning length. This limit has been previously discussed in [23].

the presence of these minimums is asymmetric especially for small $\tilde{t}_\perp$. This behavior can be understood by looking in more details at the RG equations. At a scale $l < l_{2\text{ch.}}$, where $l_{2\text{ch.}}$ is such that $t_\perp(l_{2\text{ch.}}) = \frac{\pi v_F}{a}$, the RG equations are those of the one dimensional system, and interactions in the spin sector are renormalized towards zero in the case of repulsive interactions. Only for $l > l_{2\text{ch.}}$ are interactions in the spin sector growing again to lead to the spin gap. By contrast, for attractive interactions, the interactions are always growing in the spin sector, irrespective of the strength of $\tilde{t}_\perp$. This implies that the spin gap is much weaker in the case of small $\tilde{t}_\perp$ and repulsive interactions thus making the system more sensitive to disorder. Therefore, in the case of the ladder, enhancement of localization is not determined only by the sign of interaction but also by their strength. In the case of weak interactions, the behavior is similar to the single chain case. For stronger interactions, the effect can be inverted and attractive interactions can have a delocalizing effect. Finally, for even stronger interaction, the difference between attractive and repulsive interactions becomes unobservable. It would be interesting to study how the charge stiffness is modified by disorder in these different regimes.

A problem related to the single chain to two chain crossover is the issue of confinement *i.e.* the irrelevance of single particle hopping under RG. As discussed in Section 5.5.1, the criterion for deconfinement is $E_{\text{loc.}} = t_\perp$. This criterion indeed reproduces the phase boundary between the phase III (deconfined) and IV (confined) as can be seen by comparing Figures 6 and 8. Interestingly, a kind of confinement seems to be observed in phase (IIa) as a result of attractive interaction. However, an effective two-particle hopping is known to be generated in this case [59,60] and plays the role of a Josephson coupling between the chain. Such coupling causes the formation of a gap in the transverse charge mode so that the phase (IIa) is still the SCs phase in the absence of disorder and becomes the $4k_F$ pinned CDW in the presence of disorder. Confinement of carriers by disorder is obtained in the case of strong disorder. Such a confinement has not been considered in the previous study of the spinless fermions case [40] due to a choice of large $t_\perp$. The difference in confinement is as follows. In the spinful case and for a single chain, disorder generates a spin gap in the localized phase. Thus, in the localized phase (region (IV) in Fig. 5), a gap in the single chain has to be overcome to permit single particle hopping. If one turns on a weak single particle hopping between two chains, its effect is negligible since the fields $\phi_{\rho+}$ in both chains are disordered as a result of the presence of strong disorder (this is to be contrasted with the phase IIa). In the case of spinless fermions, no spin degree of freedom is available to induce a spin gap so that the "confinement" results only from the growth of the $y_\perp$ term under RG. As one can see from this discussion, this effect is not limited to the two chain problem but is also present for any number of coupled chains. Therefore, confinement by disorder is a generic feature of coupled disordered spinful chains and should also be observable for instance with three coupled chains.

7 Conclusion

In the present paper, we have applied RG techniques to study Anderson localization in a two-chain Hubbard ladder for arbitrary ratio of $t_\perp, U, \mathcal{D}$. We have found that there were three different types of localized phases: the $4k_F$ pinned CDW (I and II) the $2k_F$ CDW$^\pi$ (III) and the decoupled single chain $2k_F$ CDW (IV). We have been able to obtain the full phase diagram of this system. We have shown that a weak interchain hopping could lead to a *reinforcement* of localization, but a strong interchain hopping resulted in a reduction of localization as discussed in [23]. The presence of $2k_F$ CDW phases should have interesting consequences on transport properties that need separate investigation. A remaining open problem is to study the generation of the $4k_F$ disorder (*i.e.* disorder that couples to the $4k_F$ CDW operator) directly from the RG equations and the resulting overall behavior of conductivity. This will be left for a future study.

We thank S. Fujimoto, T. Giamarchi, N. Kawakami, M. Tsuchiizu and H. Yoshioka for discussions. One of the authors (E.O.) is thankful for the financial support from Nagoya University where he stayed from January to March in 2001. This work was partially supported by a Grant-in-Aid for Scientific Research from the Ministry of Education, Science, Sports and Culture (Grant No.09640429), Japan.

References

1. T.M. Rice, S. Gopalan, M. Sigrist, Europhys. Lett. **23**, 445 (1993).
2. M. Fabrizio, Phys. Rev. B **48**, 15838 (1993).
3. N. Nagaosa, Sol. State Comm. **94**, 495 (1995).
4. A.M. Finkelstein, A.I. Larkin, Phys. Rev. B **47**, 10461 (1993).
5. D.V. Kveschenko, T.M. Rice, Phys. Rev. B **50**, 252 (1994).
6. H.J. Schulz, Phys. Rev. B **53**, R2959 (1996).
7. N. Nagaosa, M. Oshikawa, J. Phys. Soc. Jpn **65**, 2241 (1996).
8. L. Balents, M.P.A. Fisher, Phys. Rev. B **53**, 12133 (1996).
9. D.G. Shelton, A.M. Tsvelik, Phys. Rev. B **53**, 14036 (1996).
10. H. Yoshioka, Y. Suzumura, Phys. Rev. B **54**, 9328 (1996).
11. H. Yoshioka, Y. Suzumura, J. Low Temp. Phys **106**, 49 (1997).
12. D. Poilblanc, D.J. Scalapino, W. Hanke, Phys. Rev. B **52**, 6796 (1995).
13. C.A. Hayward *et al.*, Phys. Rev. Lett. **75**, 926 (1995).
14. H. Tsunetsugu, M. Troyer, T.M. Rice, Phys. Rev. B **49**, 16078 (1994).
15. D. Poilblanc, H. Tsunetsugu, T.M. Rice, Phys. Rev. B **50**, 6511 (1994).
16. M. Fabrizio, A. Parola, E. Tosatti, Phys. Rev. B **46**, 3159 (1992).
17. R. Noack, S. White, D. Scalapino, Phys. Rev. Lett. **73**, 882 (1994).
18. E. Dagotto, J. Riera, D. Scalapino, Phys. Rev. B **45**, 5744 (1992).
19. Y. Park, S. Liang, T.K. Lee, Phys. Rev. B **59**, 2587 (1999).
20. M. Uchara *et al.*, J. Phys. Soc. Jpn **65**, 2764 (1996).
21. T. Giamarchi, H.J. Schulz, Phys. Rev. B **37**, 325 (1988).
22. E. Orignac, T. Giamarchi, Phys. Rev. B **53**, 10453 (1996).
23. E. Orignac, T. Giamarchi, Phys. Rev. B **56**, 7167 (1997).
24. J. Akimitsu *et al.*, Physica C **263**, 475 (1996).
25. T. Osafune *et al.*, Phys. Rev. Lett. **82**, 1313 (1999).
26. T. Adachi *et al.*, Sol. State Comm. **105**, 639 (1998).
27. B. Ruzicka *et al.*, Eur. Phys. J. B **6**, 301 (1998).
28. H. Mayaffre *et al.*, Science **279**, 345 (1998).
29. T. Nagata *et al.*, Physica C **282-287**, 153 (1997).
30. T. Nagata *et al.*, Phys. Rev. Lett. **81**, 1090 (1998).
31. Y. Piskunov *et al.*, Eur. Phys. J. B **13**, 471 (2000).
32. E. Arrigoni, B. Brendel, W. Hanke, Phys. Rev. Lett. **79**, 2297 (1997).
33. S. Ijima, Nature **354**, 56 (1991).
34. A.A. Odintsov, H. Yoshioka, in *Low-Dimensional Systems: Interactions and transport properties*, Vol. 544 of *Lecture Notes in Physics*, edited by T. Brandes (Springer, Heidelberg, 2000), p. 97.
35. U. Meirav, M.A. Kastner, M. Heilblum, S.J. Wind, Phys. Rev. B **40**, 5871 (1989).
36. U. Meirav, M.A. Kastner, S.J. Wind, Phys. Rev. Lett. **65**, 771 (1990).
37. S. Tarucha, T. Saku, Y. Tokura, Y. Hirayama, Phys. Rev. B **47**, 4064 (1993).
38. O.A. Starykh, D.L. Maslov, W. Häusler, L.I. Glazman, in *Low-Dimensional Systems: Interactions and transport properties*, Vol. 544 of *Lecture Notes in Physics*, edited by T. Brandes (Springer, Heidelberg, 2000), p. 37.
39. For a review see: D. Belitz, T.R. Kirkpatrick, Rev. Mod. Phys. **66**, 261 (1994).
40. E. Orignac, Y. Suzumura, T. Giamarchi, J. Phys. Soc. Jpn **69**, 3642 (2000).
41. J. Sólyom, Adv. Phys. **28**, 209 (1979).
42. V.J. Emery, in *Highly Conducting One-Dimensional Solids*, edited by J.T. Devreese *et al.* (Plenum, New York, 1979), p. 327.
43. H. Fukuyama, H. Takayama, in *Electronic properties of inorganic quasi-oner dimensional compounds part*, edited by P. Monceau (D. Reidel Publishing Company, New York, 1985), p. 41.
44. H.J. Schulz, in *Mesoscopic quantum physics, Les Houches LXI*, edited by E. Akkermans, G. Montambaux, J.L. Pichard, J. Zinn-Justin (Elsevier, Amsterdam, 1995), p. 533.
45. J. Voit, Rep. Prog. Phys. **58**, 977 (1995).
46. Y. Suzumura, M. Tsuchiizu, G. Gruner, Phys. Rev. B **57**, R15040 (1999).
47. M. Tsuchiizu, Y. Suzumura, Phys. Rev. B **59**, 12326 (1999).
48. S. Fujimoto, N. Kawakami, Phys. Rev. B **56**, 9360 (1997).
49. H. Mori, Phys. Rev. B **58**, 12699 (1998).
50. H. Mori, Phys. Rev. B **58**, 3486 (1998).
51. N.P. Sandler, D.L. Maslov, Phys. Rev. B **55**, 13808 (1997).
52. J.L. Cardy, *Scaling and Renormalization in Statistical Physics*, *Cambridge Lecture Notes in Physics* (Cambridge University Press, Cambdridge, UK, 1996).
53. S. Fujimoto, N. Kawakami, Phys. Rev. B **54**, R11018 (1996).
54. H.J. Schulz, in *Correlated fermions and transport in mesoscopic systems*, edited by T. Martin, G. Montambaux, J. Tran Thanh Van (Éditions frontières, Gif sur Yvette, France, 1996), p. 81.
55. E. Orignac, T. Giamarchi, Phys. Rev. B **57**, 11713 (1998).
56. M. Tsuchiizu, P. Donohue, Y. Suzumura, T. Giamarchi, Eur. Phys. J. B **19**, 185 (2001).
57. K. Le Hur, Phys. Rev. B **63**, 165110 (2001).
58. T. Giamarchi, B.S. Shastry, Phys. Rev. B **51**, 10915 (1995).
59. C. Bourbonnais, in *Strongly interacting fermions and High-T_c Superconductivity*, edited by B. Douçot, J. Zinn-Justin (Elsevier, Amsterdam, 1995), p. 307.
60. J.I. Kishine, K. Yonemitsu, J. Phys. Soc. Jpn **67**, 2590 (1998).